Supporting Information for: Quantum Behavior of Water Molecules Confined to Nanocavities in Gemstone

B. P. Gorshunov, E. S. Zhukova, V. I. Torgashev, V. V. Lebedev, G. S. Shakurov, R. K. Kremer, E. V. Pestrjakov, V. G. Thomas, D. A. Fursenko, and M. Dressel

S1 Experimental Details

Beryl single crystals were grown in stainless steel autoclaves according to the regular hydro-thermal growth method at the temperature of 600°C and under pressure of 1.5 kbar by a recrystallization of natural beryl to a seed. For optical measurements a crystal of about a cubic centimeter size was x-ray oriented and cut in slices, the crystallographic c-axis was directed within the planes. This geometry allowed measuring the optical response in the two principal polarizations with the electrical vector of the probing radiation oriented parallel and perpendicular to the c-axis.

Optical measurements have been performed using two kinds of spectrometers. For infrared investigations, a standard Fourier transform spectrometer Bruker IFS-113V was used to measure the spectra of reflection and transmission coefficients, $R(\nu)$ and $Tr(\nu)$. The reflectivity spectra were recorded of samples of about 1 mm thickness. For the transmission measurements thin (about 100μm) samples were prepared. The same specimen was used to study the low frequency properties; here we employed a quasioptical spectrometer based on monochromatic and continuously frequency tunable radiation generators, that is, backward-wave oscillators [S1]. The arrangement as a Mach-Zehnder interferometer allows us to directly determine the spectra of complex dynamical conductivity $\sigma^* = \sigma_1 + \mathrm{i}\sigma_2$, dielectric permittivity $\epsilon^* = \epsilon' + \mathrm{i}\epsilon''$, etc., at frequencies from 1 cm^{-1} up to 50 cm^{-1}, in the temperature interval from 2 K to 300 K.

In order to identify water-related features in our spectra, we have performed optical experiments on dehydrated samples. In the course of the dehydration procedure, the beryl crystals were heated up to 1000°C in a vacuum for a period of 24 hours. The comparative analysis of optical spectra of samples with and without water (see Fig. S1) allowed us to unambiguously distinguish water related absorption resonances from those connected with phonons or impurities.

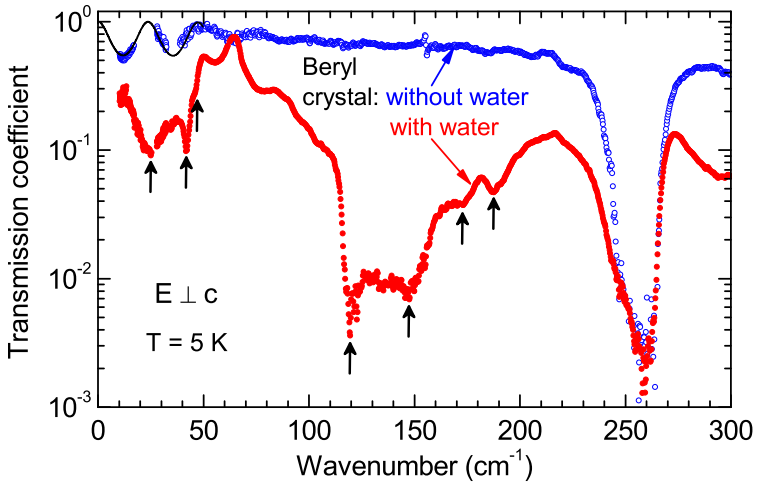

Figure S1: (Color online) Raw spectra of the transmission coefficient of a beryl crystal before (full red dots) and after dehydration (open blue dots). The 102 μm thick specimen was measured with the electric field $E \perp c$ at a temperature $T = 5$ K. The black line at low frequencies gives an example of the fit to the spectra based on Fresnel's expression [Eqs. (S1) - (S4)] for transmission of a plane-parallel layer where interference effects (Fabry-Perot resonances) lead to oscillations. The water absorption (shown by the arrows) disappears after annealing in vacuum at 1000°C for 24 hours; the phonon absorption (for instance the line at 260 cm^{-1}) remains unchanged.

S2 Data Analysis

In order to extract parameters of each resonance we have analyzed the measured $Tr(\nu)$ and $R(\nu)$ spectra using the Fresnel expressions for complex transmission Tr^* and reflection R^* coefficients of a plane-parallel layer [S2, S3]:

$$Tr^* = \frac{T_{12}T_{21}\exp\{\mathrm{i}\delta\}}{1+T_{12}T_{21}\exp\{2i\delta\}} \quad \text{and} \quad R^* = \frac{R_{12}+R_{21}\exp\{2\mathrm{i}\delta\}}{1+R_{12}R_{21}\exp\{2i\delta\}} \quad . \tag{S1}$$

Here

$$T_{pq} = t_{pq}\exp\{\mathrm{i}\phi^T_{pq}\} \quad \text{and} \quad R_{pq} = r_{pq}\exp\{\mathrm{i}\phi^R_{pq}\} \quad ; \tag{S2}$$

are the Fresnel coefficients for the interfaces "air-sample", with

$$t^2_{pq} = \frac{4(n_p^2+k_p^2)}{(k_p+k_q)^2+(n_p+n_q)^2} \quad \text{and} \quad r^2_{pq} = \frac{(n_p-n_q)^2+(k_p-k_q)^2}{(k_p+k_q)^2+(n_p+n_q)^2} \quad ; \tag{S3}$$

$$\phi^T_{pq} = \arctan\left\{\frac{k_pn_q-k_qn_p}{n_p^2+k_p^2+n_pn_q+k_pk_q}\right\} \quad \text{and} \quad \phi^R_{pq} = \arctan\left\{\frac{2(k_pn_q-k_qn_p)}{n_p^2+k_p^2-n_q^2-k_q^2}\right\} \quad . \tag{S4}$$

Here the indices $p, q = 1, 2$ denote the material: "1" corresponds to air (refractive index $n_1 = 1$, extinction coefficient $k_1 = 0$) and "2" corresponds to the sample (n_2, k_2). Furthermore $\delta = \frac{2\pi d}{\lambda}(n_2 + \mathrm{i}k_2)$, d is the sample thickness, λ is the radiation wavelength.

Most of the observed absorption resonances can be described by the regular Lorentzian expression for the complex dielectric permittivity

$$\epsilon^*(\nu) = \epsilon'(\nu) + \mathrm{i}\epsilon''(\nu) = \sum_j \frac{f_j}{\nu_j\gamma_j + \mathrm{i}(\nu_j^2-\nu^2)} \quad , \tag{S5}$$

where $\epsilon'(\nu) = n_2^2 - k_2^2$ and $\epsilon''(\nu) = 2n_2k_2$ are real and imaginary parts of $\epsilon^*(\nu)$, $f_j = \Delta\epsilon_j^*\nu_j^2$ is the oscillator strength of the jth resonance, $\Delta\epsilon_j$ is its dielectric contribution, ν_j is the resonance frequency and γ_j is the damping. For some resonance absorptions, however, we were not able to describe the shape of the curves in $Tr(\nu)$ and $R(\nu)$ spectra with the Eq. (S5). These are in particular the absorption lines located at $120 - 160$ cm^{-1}. A satisfactory description could only be reached by the expression for coupled Lorentzians where the complex dielectric permittivity is written as [S4]:

$$\epsilon^*(\nu) = \frac{f_1(\nu_2^2-\nu^2+\mathrm{i}\nu\gamma_2) + f_2(\nu_1^2-\nu^2+\mathrm{i}\nu\gamma_1) - 2\sqrt{f_1f_2}(\alpha+\mathrm{i}\nu\delta)}{(\nu_1^2-\nu^2+\mathrm{i}\nu\gamma_1)(\nu_2^2-\nu^2+\mathrm{i}\nu\gamma_2) - (\alpha+\mathrm{i}\nu\delta)^2} \tag{S6}$$

where $j = 1, 2$; $f_j = \Delta\epsilon_j\nu_j^2$ is the oscillator strength of the jth Lorentzian with ν_j being the eigenfrequency, α is the real and δ is the imaginary coupling constants.

We have fitted the infrared $Tr(\nu)$ and $R(\nu)$ spectra with the expressions (S1) through (S6) in combination with the ac conductivity and permittivity spectra measured directly at the terahertz range. In order to distinguish water-related absorptions from phonon resonances, the same procedure was applied to the spectra of dehydrated samples. The phonon resonances have been subtracted from the spectra by setting corresponding oscillator strengths in Eqs. (S5) and (S6) to zero. This allows us to eventually identify the water-related absorption lines for both principle polarizations.

S3 Mode Assignment

The eigenfrequencies and other parameters of the infrared ground-band transitions and transitions from the ground band to the translation and the libration bands are summarized in Table S1 for the $E \perp c$ polarization. The corresponding energies of the transitions are also indicated. The wide bump near 25 cm^{-1} in the conductivity spectrum of Figs. 2 and 5 can be ascribed to transitions between the states within the ground band. We were not able to satisfactorily reproduce the bump with one or more simple Lorentzians [Eq. (S5)] but only with a set of coupled Lorentzians [Eq. (S6)]. This complicated shape is explained by possible interconnection between populations of ground-band energy levels and also by an inhomogeneous broadening of the levels that is related to the electric field of charged impurities (metallic ions) present in the sample. The electric field randomly shifts the energy levels of the ground band due to interaction with the water molecule via its dipole moment.

Table S1: Parameters obtained from the Lorentz fit [Eq. (S5)] of the type-I water related THz and far-infrared modes observed in beryl for polarization $E \perp c$ at $T = 5$ K. ν_0 denotes the eigenfrequency, f the oscillator strength (intensity), and γ the damping; $\mathcal{E}$ denotes the corresponding energy of the transition in meV. Stars mark the values obtained using the model of coupled Lorentzians Eq. (S6).

THz and sub-THz band (intra-ground-band transitions)				
$\mathcal{E}$ (meV)	ν_0 (cm^{-1})	f (cm^{-2})	γ (cm^{-1})	Assignment $(n,m) \to (n,m)$
1.33	10.7 *	106 *	12 *	$(1,0) \to (1,1)$
3.21	25.9 *	1 770 *	25 *	$(1,1) \to (1,2)$
5.21	42	74	1.5	?
5.82	47	134	6	?

Far-infrared translation band (transitions between ground-band and translational band)				
$\mathcal{E}$ (meV)	ν_0 (cm^{-1})	f (cm^{-2})	γ (cm^{-1})	Assignment $(n,m) \to (n,m)$
14.01	113	3 320	43	$(1,1) \to (2,0)$
14.51	117 *	2 960 *	8 *	$(1,2) \to (2,1)$
18.35	148 *	1 860 *	34 *	$(1,0) \to (2,1)$
21.33	172	900	19	$(1,3) \to (2,2)$
23.44	189	780	15	$(1,1) \to (2,2)$
27	218	1300	42	$(1,2) \to (2,3)$

Far-infrared libration band (transitions between ground-band and librational band)				
$\mathcal{E}$ (meV)	ν_0 (cm^{-1})	f (cm^{-2})	γ (cm^{-1})	Assignment $(n,m) \to (n,m)$
36.21	292	2 020	34	$(1,1) \to (2,0)$
46.38	374	13 220	15	$(1,2) \to (2,1)$
53.32	430	10 750	14	$(1,0) \to (2,1)$
56.05	452	26 600	8	$(1,3) \to (2,2)$
56.92	459	10 110	5.9	$(1,1) \to (2,2)$
58.53	472	42 870	9	$(1,2) \to (2,3)$

Table S2 summarizes the parameters of the water absorption lines in beryl observed for $E \perp c$ in the infrared range around the intramolecular vibrations ν_1, ν_2 and ν_3 of H_2O (Fig. 3). Since the infrared satellite resonances are combinations of these internal modes ν_i with lower frequency excitations ν_j, we also present the correspondent differences in Table S2. Most of the differential frequencies fall below approximately 200 cm^{-1} correlating well with the peak positions related to the transitions to the translational band (Tab. S1). This suggests that the intramolecular modes of H_2O molecule most easily couple to its translational vibrations [S5]. There are few rather intensive infrared resonances that produce differential frequencies above $200-300$ cm^{-1}, up to about 530 cm^{-1}. They correspond to excitations within the librational band; this suggests a coupling of H_2O internal modes to the rotational degrees of freedom. For several infrared absorptions there are no counterparts in the far-infrared or THz-subTHz ranges, presumably due to their low intensity and/or large damping.

Table S2: Parameters and assignments of water-related infrared modes in beryl obtained from the Lorentz fit [Eq. S5)] for the polarization $E \perp c$ at $T = 5$ K. As in Table S1, $\mathcal{E}$ denotes the energy of the transition, ν_0 the corresponding eigenfrequency, f is the oscillator strength, and γ the damping. The bold lines correspond to the internal vibrations ν_1, ν_2 and ν_3 of H_2O. Differences between positions of ν_1, ν_2 and ν_3 and the observed modes are also presented.

Infrared modes around of internal H_2O mode $\nu_2 = 1595$ cm^{-1}				
$\mathcal{E}$ (meV)	ν_0 (cm^{-1})	f (cm^{-2})	γ (cm^{-1})	$\lvert\nu_2^I - \nu_0\rvert$ (cm^{-1})
197.3	**1 591**	**695**	**7.4**	ν_2, Water-I
197.7	1 594	84	2.6	3
198.0	1 597	215	5	6
199.9	1 612	857	29	21
202.7	1 634	190	25	43
212.0	1 710	29	12	119

Infrared modes around the internal H_2O modes $\nu_1 = 3657$ cm^{-1} and $\nu_3 = 3756$ cm^{-1}					
$\mathcal{E}$ (meV)	ν_0 (cm^{-1})	f (cm^{-2})	γ (cm^{-1})	$\lvert\nu_1^I - \nu_0\rvert$ (cm^{-1})	$\lvert\nu_3^{II} - \nu_0\rvert$ (cm^{-1})
389.9	3 144	32	14	461	528
446.2	3 598	80	12	7	74
446.9	**3 604**	**277**	**0.8**	ν_1, Water-I	
449.5	3 625	70	52	20	47
453.7	3 659	57	4	54	13
454.3	3 664	270	8	59	8
454.8	3 668	70	4.4	63	4
455.1	3 670	15	1.8	65	2
455.3	**3 672**	**342**	**6.6**	ν_3, Water-II	
455.7	3 675	36	3	71	3
456.0	3 677	225	5.5	73	5
457.1	3 686	136	5	82	14
458.7	3 699	20	3	95	27
461.8	3 724	144	20	120	52
463.9	3 741	4	7	137	69
465.4	3 753	183	22	149	81
479.4	3 866	40	13	262	194
483.0	3 895	250	30	291	223
486.1	3 920	60	15	316	248
653.5	5 270	50	7	1 665	1 598

In contrast to the $E \perp c$ polarization, the experimental spectra for $E \parallel c$ are rather poor: only two resonances are seen at 5 K in the far-infrared and THz frequency range (Fig. 2), and just two satellite peaks accompany the H_2O intramolecular modes (Fig. 3) with their parameters given in Table S3.

Table S3: Parameters obtained from the Lorentz fit [Eq. (S5)] of the type-I water related modes observed in beryl for polarization $E \parallel c$ at $T = 5$ K. ν_0 denotes the eigenfrequency, f the oscillator strength (intensity), and γ the damping; $\mathcal{E}$ denotes the corresponding energy of the transition in meV. For the infrared range, spectral distances are presented with respect to the positions of the intramolecular water vibrations; i.e. differences between of the observed modes and ν_1, ν_2 and ν_3.

THz and sub-THz band				
$\mathcal{E}$ (meV)	ν_0 (cm^{-1})	f (cm^{-2})	γ (cm^{-1})	Assignment
10.91	88	200	4	Water-I. Translational mode
19.6	158	2 780	22	Water-I. Librational mode

Infrared modes around the internal H_2O mode $\nu_2 = 1595$ cm^{-1}				
$\mathcal{E}$ (meV)	ν_0 (cm^{-1})	f (cm^{-2})	γ (cm^{-1})	$\lvert\nu_2^{II} - \nu_0\rvert$ (cm^{-1})
197.2	1 590	21	1.7	32
201.1	1 622	12 450	0.7	ν_2, Water-II
220.7	1 780	82	37	158

Infrared modes around the internal H_2O modes $\nu_1 = 3657$ cm^{-1} and $\nu_3 = 3756$ cm^{-1}				
$\mathcal{E}$ (meV)	ν_0 (cm^{-1})	f (cm^{-2})	γ (cm^{-1})	Assignment
446.3	3 599	955	5.5	ν_1, Water-II
458.3	3 696	490	5.6	ν_3, Water-I
653.4	5 269	95	2.9	$\nu_1 + \nu_2 = 5\,221$ cm^{-1} Water-II

References

[S1] Gorshunov, B.; Volkov, A.; Spektor, I.; Prokhorov, A.; Mukhin, A.; Dressel, M.; Uchida, S.; Loidl, A. *Int. J. of Infrared and Millimeter Waves* **2005**, *26*, 1217-1240.

[S2] Born, M.; Wolf, E. *Principles of Optics*, 7th edition, Cambridge University Press, Cambridge, **1999**.

[S3] Dressel M.; Grüner, G. *Electrodynamics of Solids*, Cambridge University Press, Cambridge, **2002**.

[S4] Barker, A. S.; Hopfield, J. J. *Phys. Rev.* **1964**, *135*, A1732-A1737.

[S5] Kolesov, B. A.; *J. Struct. Chem.* **2006**, *47*, 21-34.